One- and Two-Photon Induced Photochemistry of Fe(CO)5: Insights from Coupled Cluster Response Theory

CHEMISTRY OF LIGHT INTERACTION

CHEMPHOTOCHEM

ACROSS THE WHOLE SPECTRUM

Accepted Article

Title: One- and Two Photon Induced Photochemistry of Fe(CO)5: Insights from Coupled Cluster Response Theory

Authors: Thomas Malcomson, Russell Mckinlay, and Martin J. Paterson

To be cited as: *ChemPhotoChem* 10.1002/cptc.201900111

Link to VoR: http://dx.doi.org/10.1002/cptc.201900111

A Journal of

ChemPubSoc Europe

WILEY-VCH

www.chemphotochem.org

WILEY-VCH

ARTICLE

One- and Two-Photon Induced Photochemistry of $Fe(CO)_5$: Insights from Coupled Cluster Response Theory

Thomas Malcomson[a], Russell G McKinlay[a], and Martin J. Paterson*[a]

Abstract: We present here the first comprehensive study of the one- and two-photon absorption of $Fe(CO)_5$ utilising a hierarchy of linear- and quadratic-response coupled cluster (LR- and QR-CC) methodologies to provide an in-depth characterisation, as well as potential energy curves for axial and equatorial bond dissociations, highlighting the state crossings leading from the bright $1A_2$" state through to the dissociative 1E' state. We have characterised a range of MLCT and LF states that are in agreement with both previous studies and experiment, including the identification of a series of E' states that present Rydberg character in the 5.9-7.2 eV region. Due to the rapid excited state dissociation of $Fe(CO)_5$ through the low lying 1E' and 2E" ligand-field states, we have also included an LR-CCSD analysis of the major dissociative product, $Fe(CO)_4$. Analysis of the C_{2v} geometry of $Fe(CO)_4$ reveals four accessible ligand field states at 1.085, 1.684, 1.958, and 2.504 eV respectively, reinforcing the highly unstable nature of $Fe(CO)_4$ along with a strong MLCT band between 4.300 and 5.573 eV. This band overlaps with one in the spectra of $Fe(CO)_5$ suggesting that full fragmentation could proceed by two paths: two-photon excitation leading to dissociation, or through sequential one-photon absorption events, the first causing dissociation to and the second initiating further fragmentation of the complex.

Introduction

Transition metal carbonyls are some of the most intensely studied organometallic compounds with much attention paid to their photochemistry.[1, 2] Early work on the photochemical activity of metal carbonyls focused on their electronic spectroscopy[3-5] and dissociative reactivity,[6, 7] however more recent works have used laser-based pump/probe spectroscopic techniques which show that the formation of the photoproducts of some metal carbonyls can occur on a femtosecond (fs) timescale.[8-14] Indeed, the relatively simple structures of such transition metal carbonyls belie complex photodissociation dynamics, including evidence of emerging Jahn-Teller induced phenomena in both the early and latter stages of their photodissociation mechanisms.[13-18] In parallel with the development of experimental techniques, theoretical methodologies such as time-dependent density functional theory (TD-DFT), coupled cluster (CC) theory,[19] multi-configurational complete active space self-consistent field (CASSCF) and complete active space second order perturbation (CASPT2) theories[20-24] have all successfully been applied to the analysis of metal carbonyls photochemistry. Such computational approaches now allow for a rich interpretation of the detailed coupled multi-state photo-dynamics that can occur.

Coupled cluster response theory has emerged as an outstanding benchmarking method for excited electronic states.[25-29] This is due to the systematic treatment of electron correlation in the reference state, correct to a given order in the fluctuation potential, which then allows the same high level of accuracy for excited state energies and properties through the appropriate response function. For transition metal complexes CC response theory has many attractive features in that that it treats excited-state (multi-configurational) mixing very well, it is systematically improvable, and many states can be computed via the response function which is extremely useful given the very high density of electronic states). The subject of this study is the binary carbonyl $Fe(CO)_5$ which makes an excellent benchmarking organometallic molecule for CC response theory by virtue of a closed shell ground state and a relatively high symmetry. This system will add to the few benchmarks available in this area.[20, 30] Furthermore, CC response theory readily allows for non-linear optical properties such as two-photon absorption,[29] for which some unassigned experimental data exists for $Fe(CO)_5$.

The electronic spectrum of $Fe(CO)_5$ in the gas phase has been reported by both Marquez[22] and Kotzian.[31] The UV

[a] Institute of Chemical Sciences, Heriot-Watt University, Edinburgh, EH4 4AS, UK.
* Corresponding author

spectrum reported in Ref. [31] is dominated by two bands at 5.0 eV and 6.2 eV and show a common feature of most transition metal carbonyl electronic spectra, namely a broad, featureless spectrum with a large density of excited electronic states. We will briefly review previous computational work looking at the electronic spectroscopy and photochemistry. Early INDO/S calculations were used to assign the spectrum and concluded that the spectrum is dominated by metal-to-ligand charge transfer (MLCT) transitions. CASSCF methods have been applied to the spectroscopy of $Fe(CO)_5$ in Ref. [22] with the vacuum UV spectrum (210-110 nm) investigated, including analysis of some Rydberg states. Two Rydberg series were found between 6.14 - 7.66 eV which corresponds to excitation from the 3d shell to 4s,4p or 4d orbitals. The lowest dipole allowed state they observed was of $^1E'$ symmetry with an excitation energy of 3.54 eV. Multi-reference configuration interaction (MR-CI) methods were used to look at the lowest excited states (below 5.57 eV).[24] They found a high density of states in the region between 3.09-5.57 eV but only three allowed transitions (2 $^1E'$ and 1 $^1A_2''$). The allowed transitions were found to have excitation energies of 3.34 eV ($^1E'$), 4.58 eV ($^1A_2''$) and 4.95 eV ($^1E'$). These were believed to be the states responsible for observed photochemistry from an earlier laser photodissociation study of the fragmentation and molecular dynamics of $Fe(CO)_5$.[32] CASPT2 has been applied by Pierloot et al[33] in which they compute ligand-field (LF) and charge transfer (CT) states of singlet and triplet E' and E'' symmetry. They observe that the lowest energy singlet ligand field states compare favourably to the shoulder at 4.3 eV in the experimental spectrum[31] and that addition of dynamic correlation has the effect of lowering the excitation energies of the states studied 0.1 to 2 eV compared to CASSCF values. This is most notable in the allowed CT state where the difference between in excitation energy was 1.7 eV.

There have been a number of experimental studies relating to $Fe(CO)_5$ reactive photochemistry. In addition to the work in Ref. [34] Seder also looked at the laser photolysis of $Fe(CO)_5$.[35] Both studies investigated one-photon absorption using 352 nm, 248 nm and 193 nm light and exhibit a high degree of fragmentation from the parent molecule, leading to a sequential fragmentation mechanism being proposed. With the development of ultrafast (fs) laser experiments new information became available regarding the photodissociation of $Fe(CO)_5$. Bañares *et al* [8] were the first to report the use of femtosecond laser pulses with two-photon pumping at 400 nm and non-resonant ionisation at 800 nm with a time-of-flight (TOF) mass spectrometer to measure the appearance time of various $Fe(CO)_x$ fragments. They demonstrated that $Fe(CO)_4$ appears within 20±5 fs, some Fe(CO) is formed within 100 fs, and total dissociation by 230 fs. They proposed a mechanism for CO loss in terms of an $Fe(CO)_5$ transition state via a concerted mechanism. Ultrafast electron diffraction showed that the dissociation is complete in under 10 ps showing major products of $Fe(CO)_2$, Fe(CO) and Fe, with no observed change in their diffraction data beyond 270 ps[9, 36]. Further electron diffraction reports an accurate structure for the key intermediate $Fe(CO)_4$.[37] It was concluded that $Fe(CO)_4$ is formed in under 200 ps in the singlet $^1A_1$ state as opposed to the $^3B_2$ state, and that the subsequent reaction path would be that of the singlet manifold. This singlet pathway was also argued by Trushin[16] who used a UV laser to irradiate $Fe(CO)_5$ at 267 nm coupled to a TOF analysis of photofragments. They proposed a complex pathway following photoexcitation in which a metal ligand charge transfer (MLCT) state is initially populated, switching state to a dissociative LF state, and the formation of $Fe(CO)_4$ in the $^1A_1$ ground state in under 50 fs. Due to the number of degenerate states they believe a chain of Jahn-Teller induced conical intersections are present in this process, with further work showing similar behaviour in other metal carbonyls.[15, 17] The structure of $Fe(CO)_4$ and how it is formed is a hotly debated research topic (see for example Ref. [38]).

The work highlighted above shows some of the features and open-issues related to iron carbonyl photochemistry (these also allying in general to a wide range of metal carbonyls). It is apparent that understanding the nature of states populated and how they evolve in the first stage of the photodissociation is key to interpreting this process. A common feature of all previous computation work on $Fe(CO)_5$ excited electronic states is that only a limited number of states were calculated, and there were challenges to treat all states in a balanced manner. Coupled cluster methods have been seeing increasing use in recent years in the area of electronic spectroscopy and have been successfully applied to a range of organic species[21-24] with the closely related equation-of-motion CC (EOM-CCSD) method applied to the one photon absorption electronic spectrum of $Cr(CO)_6$.[15-19, 39] These methods allow excited states to mix freely at the correlated level, meaning they treat all excited states on an equal footing with no need to perform different calculations for different types of excited states.

The present study seeks to apply such correlated many-body approaches to both the one- and two-photon absorption of

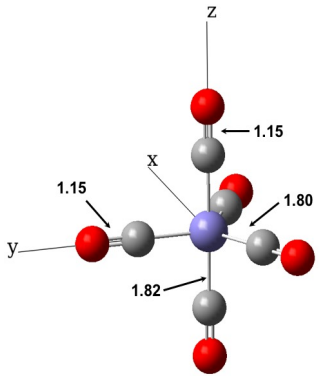

Figure 1: *Trigonal pyramid equilibrium geometry of $Fe(CO)_5$ (D_{3h} symmetry). Bond lengths in Å. Cartesian axes used to label orbitals.*

$Fe(CO)_5$ using a hierarchy of coupled cluster response theory methods (CCS, CC2, and CCSD). The assignment of the spectrum is still somewhat controversial, and is not helped by the poor resolution of the experimental spectrum with its large density of states. A fuller balanced account of the excited state behaviour is necessary to aid identification of states which have a role in the photochemical process ranging from initial vertical excitation in the Franck-Condon region, through ejection of one CO ligand, including any early time dynamical state switches.[16] It has also been shown that absorption of two photons can trigger ultrafast photochemistry in $Fe(CO)_5$.[25] However there may be subtle differences between the two processes such as the involvement of different degenerate states and reactive intermediates due to the predicted density of states in the complex. A summary of computational details is given at the end of this paper.

Results and Discussion

The optimised D_{3h} geometry of trigonal bipyramid $Fe(CO)_5$ is shown in figure 1 agrees favourably with a range of experimental geometries[40, 41] leading to the conclusion that the

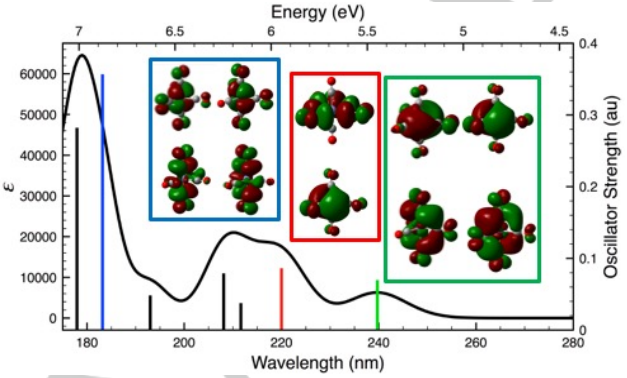

Figure 2: *LR-CCSD one-photon absorption spectra of d^8 $Fe(CO)_5$; bright states corresponding to each spectral feature shown as sticks; inlaid boxes show the hole (bottom) to particle (top) transitions for $1A_2''$ (green), $3E'$ (red), and $2A_2''$ (blue) states..*

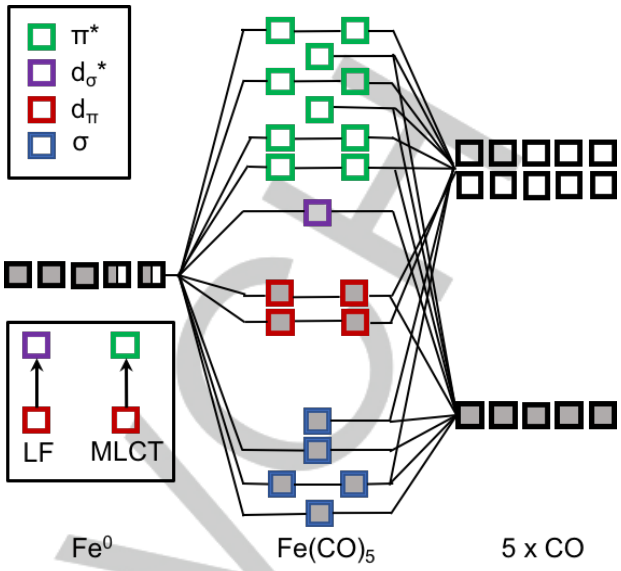

Figure 3*: Qualitative molecular orbital diagram of d^8 $Fe(CO)_5$ highlighting dominant orbital transitions in MLCT and LF states.*

CCSD optimised geometries perform well and that any effects caused by differences in geometry should be minimal, a property observed in the study of other, similar species. [30, 42, 43] A lack of accuracy caused by the size or quality of the basis set used should not be present here as a basis set of equivalent size was applied to a similar system elsewhere[19] for the one photon absorption spectrum of $Cr(CO)_6$ with no negative effects on the quality of the results. Correlation effects are also very high in this complex, evident in the mixed nature of the states presented in table 1. This shows that highly correlated methods such as QR-CCSD are needed to describe the excited states of $Fe(CO)_5$ accurately. This tends to be a very common feature in the spectroscopy of transition metal carbonyl complexes, whereby they contain a large density of excited state in a relatively small spectral range, each of a different chemical character. Within this selection of states, from the singlet A_1' ground state of $Fe(CO)_5$, electronic dipole transitions are symmetry allowed to states of E' and A_2'' symmetry, while transitions to states of other symmetries are forbidden.

Figure 2 shows the calculated one-photon absorption spectrum of $Fe(CO)_5$ using linear response CCSD (experimental spectra can be found within references 22 and 31), with the excitation energies and oscillator strengths shown in table 1, with each of the principle transitions reported possessing a weight of over 50%. The lowest excited state is a near-dark LF state of 1E´ symmetry at 4.409 eV. This compares with 3.55 eV in the previous CASSCF CCI work. We state here that this state is “near-dark” due to a very low oscillator strength, formally

noted as 0.0000 in table 1, when it is actually 0.0000065, leading a very weak allowed transition. Tables 2 and 3 show these for different CC response methods in the hierarchy for both one- and two-photon absorption. As can be seen in both tables 2 & 3, while CCS and CCSD methodologies show, in general, a good agreement in the ordering of states, there are errors >1eV in excitation energy. CC2 however shows serious errors regarding both energetics, relative state-ordering, and transition moments (bright vs dark states, e.g. 3E' and $1A_1$' in table 2). This has been observed previously for CC2 in certain transition metal compounds, including TiO_2,[43] $Ni(CO)_4$,[42] and MnO_4^- [30]. This problem, sometimes observed for CC2, for transition metal systems has been attributed to the large T_1 amplitudes which are used as similarity transform operators to ensure that the singles are treated at zeroth order both with and without the external field perturbation.[30, 44]

Figure 3 shows a qualitative molecular orbital (MO) diagram of $Fe(CO)_5$ at a trigonal bipyramid geometry (D_{3h} symmetry). This highlights the dominant single-electron transitions from the highest occupied d-orbitals to the d_z^2 leading to LF states, and a very large number of MLCT transitions to the many low-lying localised π* ligand orbitals (formed as symmetry adapted linear combinations of CO p_π orbitals). It should be noted however that the D_{3h} symmetry allows some mixing between p- and d-orbitals in the degenerate irreducible representations (irreps) so the orbitals do not have entirely pure character.

There are three metal centred ligand field states that could correspond to the first shoulders of the experimental spectrum which includes the $1A_2$" state, an MLCT state which is an allowed state and has an associated oscillator strength along with the 3E' and $2A_2$" states which are not symmetry allowed. The next experimental band (medium intensity) is believed to be of charge transfer character and could be assigned to the 3E´, 4E´, and 5E' states which are all allowed and have associated oscillator strengths given in table 1, with the 5E' state showing s-Rydberg character. The last feature of the experimental spectrum is the intense band at 6.19 eV and is again believed to be due to charge transfer states with the $2A_2$" state in this region showing a large oscillator strength at LR-CCSD levels of theory. There are two further Rydberg-type transitions in the 7E' and $2A_1$' states at 6.968 eV and 7.152 eV. Identification of these Rydberg states show agreement with the first Rydberg band observed in ref [22], corresponding to transitions from the 3d to 4s (5E'), 4p (7E'), and 4d ($2A_1$') orbitals, with the second predicted Rydberg band laying just outside of our energetic cut off between 7.94 and 8.90 eV. In

Table 1: *LR-CCSD excited singlet states for $Fe(CO)_5$.*

State	Character	Excitation Energy (eV)	Oscillator Strength (au)
1E'	LF ($3d_{xy}^{\ddagger} \rightarrow 3dz^2$) / ($3d_{x^2-y^2}^{\ddagger} \rightarrow 3dz^2$)	4.409	0.0000
$1A_1$"	MLCT ($3d_{xy}^{\ddagger} \rightarrow$ eq π*) / ($3d_{x^2-y^2}^{\ddagger} \rightarrow$ eq π*)	4.614	0.0000
1E"	MLCT ($3d_{xy}^{\ddagger} \rightarrow$ eq π*) / ($3d_{x^2-y^2}^{\ddagger} \rightarrow$ eq π*)	4.775	0.0000
$1A_2$'	MLCT ($3d_{xy}^{\ddagger} \rightarrow$ ax π*‡‡) / ($3d_{x^2-y^2}^{\ddagger} \rightarrow$ ax π*‡‡)	5.089	0.0000
2E'	MLCT ($3d_{xy}^{\ddagger} \rightarrow$ ax π*‡‡) / ($3d_{x^2-y^2}^{\ddagger} \rightarrow$ ax π*‡‡)	5.126	0.0000
$1A_2$"	MLCT ($3d_{xy}^{\ddagger} \rightarrow$ eq π*) / ($3d_{x^2-y^2}^{\ddagger} \rightarrow$ eq π*)	5.172	0.0696
2E"	LF ($3d_{xz} \rightarrow 3dz^2$) / ($3d_{yz} \rightarrow 3dz^2$)	5.274	0.0000
3E"	MLCT ($3d_{xz} \rightarrow$ eq π*) / ($3d_{yz} \rightarrow$ eq π*)	5.302	0.0000
3E'	MLCT ($3d_{xy}^{\ddagger} \rightarrow$ eq π*) / ($3d_{x^2-y^2}^{\ddagger} \rightarrow$ eq π*)	5.636	0.0862
$2A_2$'	MLCT ($3d_{xy}^{\ddagger} \rightarrow$ eq π*) / ($3d_{x^2-y^2}^{\ddagger} \rightarrow$ eq π*)	5.648	0.0000
4E'	MLCT ($3d_{xy}^{\ddagger} \rightarrow$ eq π*‡‡) / ($3d_{x^2-y^2}^{\ddagger} \rightarrow$ eq π*‡‡)	5.858	0.0375
5E'	MLCT ($3d_{xy}^{\ddagger} \rightarrow$ s-Ryd)	5.958	0.0790
$1A_1$'	MLCT ($3d_{xz} \rightarrow$ ax π*‡‡) / ($3d_{yz} \rightarrow$ ax π*‡‡)	6.033	0.0000
$3A_2$'	MLCT ($3d_{xz} \rightarrow$ ax π*‡‡) / ($3d_{yz} \rightarrow$ ax π*‡‡)	6.219	0.0000
$2A_1$"	MLCT ($3d_{xz} \rightarrow$ ax π*‡‡) / ($3d_{yz} \rightarrow$ ax π*‡‡)	6.274	0.0000
4E"	MLCT ($3d_{xz} \rightarrow$ ax π*‡‡) / ($3d_{yz} \rightarrow$ ax π*‡‡)	6.318	0.0000
6E'	MLCT ($3d_{xz} \rightarrow$ ax π*‡‡) / ($3d_{yz} \rightarrow$ ax π*‡‡)	6.424	0.0482
$2A_2$"	MLCT ($3d_{xz} \rightarrow$ ax π*‡‡) / ($3d_{yz} \rightarrow$ ax π*‡‡)	6.768	0.3568
$2A_1$"	MLCT ($3d_{xy}^{\ddagger} \rightarrow$ eq/ax π*) / ($3d_{x^2-y^2}^{\ddagger} \rightarrow$ eq/ax π*)	6.804	0.0000
5E"	MLCT ($3d_{xz} \rightarrow$ eq π*)	6.808	0.0000
$3A_1$"	MLCT ($3d_{xz} \rightarrow$ eq π*‡‡) / ($3d_{yz} \rightarrow$ eq π*‡‡)	6.878	0.0000
7E'	MLCT ($3d_{yz} \rightarrow$ ax π*‡‡) / ($3d_{yz} \rightarrow$ p-Ryd)	6.968	0.2821
6E"	MLCT ($3d_{xy}^{\ddagger} \rightarrow$ eq/ax π*) / ($3d_{x^2-y^2}^{\ddagger} \rightarrow$ eq/ax π*)	7.001	0.0000
$2A_1$'	MLCT ($3d_{xy}^{\ddagger} \rightarrow$ d-Ryd (valence mixed)) / ($3d_{x^2-y^2}^{\ddagger} \rightarrow$ p-Ryd)	7.152	0.0000
$3A_2$"	MLCT ($3d_{xz} \rightarrow$ eq π*‡‡) / ($3d_{yz} \rightarrow$ eq π*‡‡)	7.169	0.0266

‡ indicates an orbital of predominantly *d* character containing significant π* mixed character
‡‡ indicates an orbital of predominantly π* character containing significant *d* mixed character

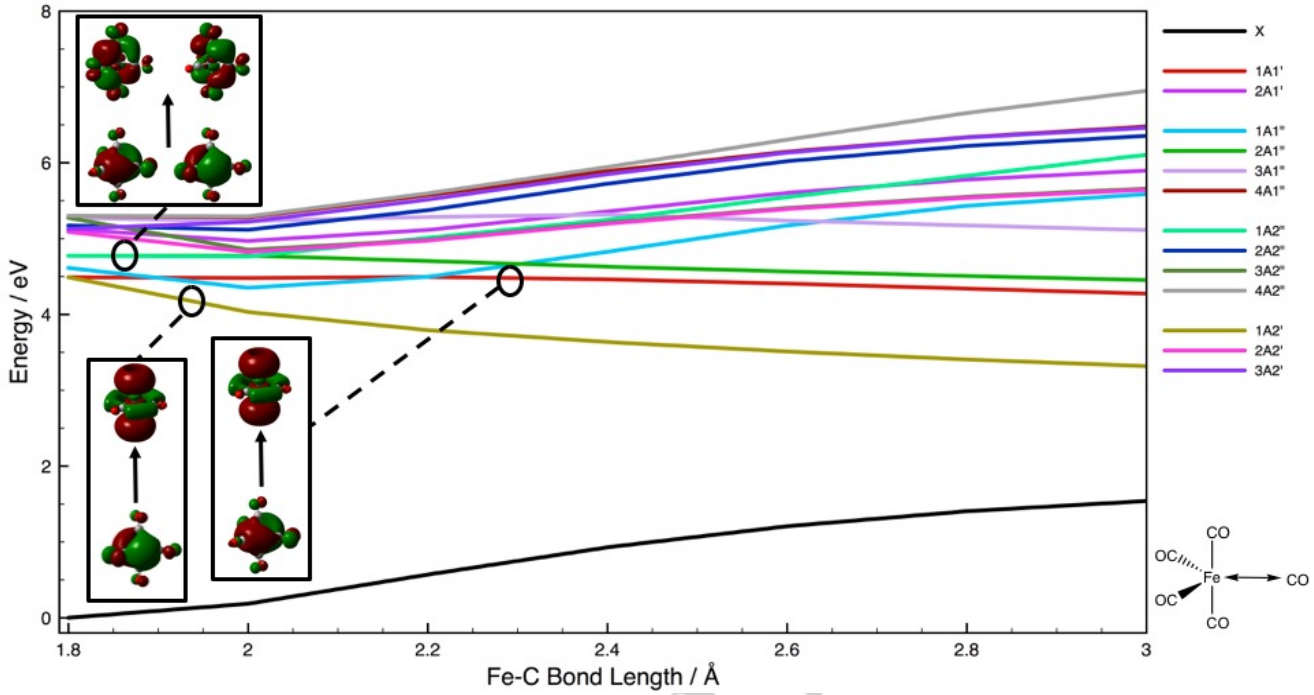

Figure 4: *Rigid LR-CCSD scan of $Fe(CO)_5$ excited singlet states as a function of the equatorial Fe-C bond stretch; inlaid are orbital transitions relating to the $1A_2$" state (top), $1A_2$' state (bottom, left), and $1A_1$" (bottom, right) states.*

between these one-photon allowed states there are a large number of symmetry forbidden states of both charge transfer and ligand field character. In previously discussed work of Trushin[16] they believe that after excitation at 267 nm an MLCT state is initially populated followed by a process of photodissociation in the singlet manifold involving two Jahn-Teller induced conical intersections involving the 1E´ and 2E´ excited states coupled through e vibrations. These include the symmetric equatorial, and symmetric equatorial-axial bends, an asymmetric equatorial-axial bend coupled to an equatorial bond stretch, a symmetric equatorial bend coupled to an equatorial bond stretch, as well as a high energy asymmetric equatorial bond stretch, temporarily

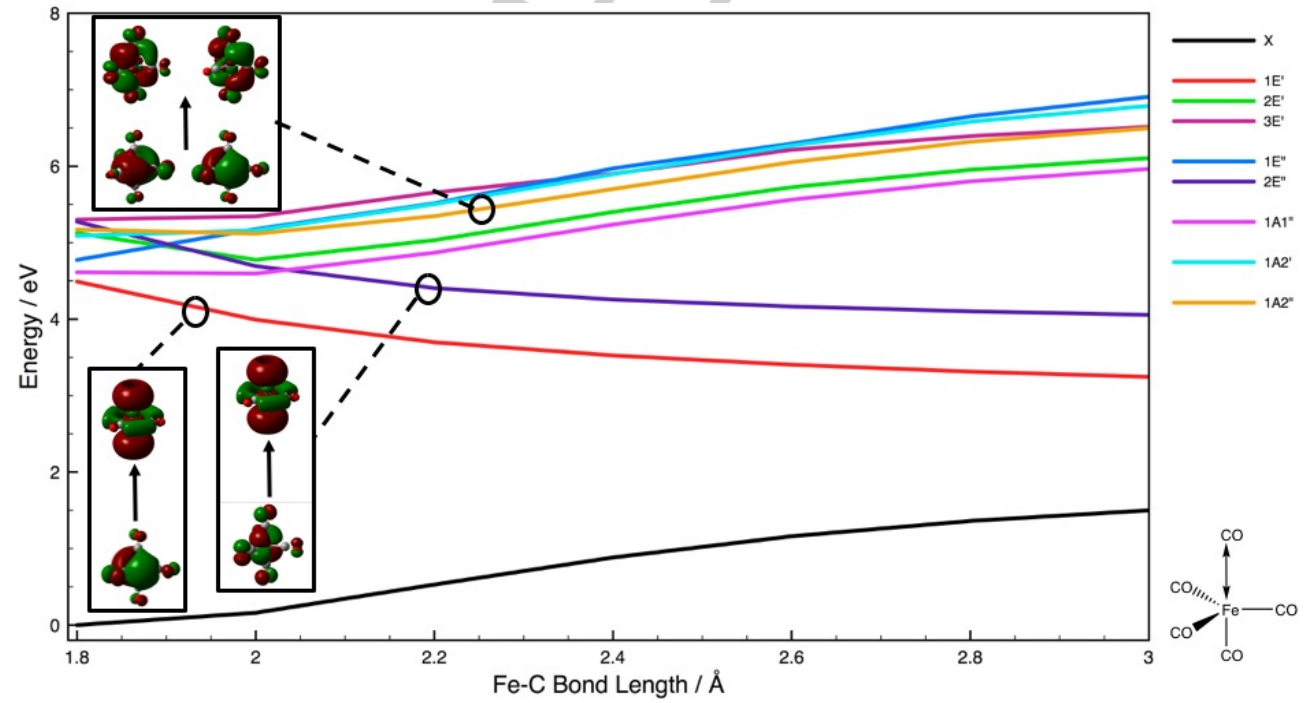

Figure 5: *Rigid LR-CCSD scan of $Fe(CO)_5$ excited singlet states as a function of the axial Fe-C bond stretch; inlaid are the orbital transitions relating to the $1A_2$" state (top), 1E' state (bottom, left), and 1E" state (bottom, right) states.*

Table 2: *Coupled cluster response hierarchy for one-photon excited singlet states of $Fe(CO)_5$.*

LR-CCS			LR-CC2			LR-CCSD		
State	Excitation Energy (eV)	Oscillator Strength (au)	State	Excitation Energy (eV)	Oscillator Strength (au)	State	Excitation Energy (eV)	Oscillator Strength (au)
1E’	4.038	0.0433	1E’	3.440	0.1629	1E’	4.362	0.0000
$1A_1$”	3.847	0.0000	$1A_1$”	4.237	0.0000	$1A_1$”	4.596	0.0000
1E”	3.843	0.0000	1E”	3.416	0.0000	1E”	4.766	0.0000
$1A_2$’	3.833	0.0000	$1A_2$’	3.556	0.0000	$1A_2$’	5.071	0.0000
2E”	4.199	0.0000	2E”	4.161	0.0000	2E”	5.121	0.0003
2E’	4.271	0.1106	2E’	3.519	0.0052	2E’	5.156	0.0694
$1A_2$”	4.751	0.1373	$1A_2$”	3.833	0.4655	$1A_2$”	5.158	0.0000
3E”	6.409	0.0000	3E”	4.177	0.0000	3E”	5.306	0.0000
$2A_2$’	6.524	0.0000				$2A_2$’	5.636	0.0000
3E’	6.810	0.0336	3E’	3.731	0.0844	3E’	5.640	0.0000
$1A_1$’	5.697	0.0000	$1A_1$’	3.563	0.0000	$1A_1$’	5.645	0.0909
$2A_1$’	6.957	0.0837				$2A_1$’	5.849	0.0570
$2A_1$”	5.962	0.0000				$2A_1$”	6.261	0.0000
$2A_2$”	6.278	0.0593				$2A_2$”	6.322	0.0000
			4E’	4.065	0.0433			
			4E”	4.186	0.0000			

crossing over to the $1A_2$” state before returning to the repulsive ligand field 1E´ state and proceeding to eject a CO ligand to produce vibrationally hot $Fe(CO)_4$ in its lowest energy singlet state. However also note that the strongly repulsive ligand field state, which is believed to be the cause of CO ejection, could be higher in energy but the result of the process would remain unchanged. We observe that there are indeed higher energy ligand field states in the spectrum which could be responsible for this behaviour, such as the 2E” state at 5.274 eV, along with the predominantly MLCT $1A_2$” state at 5.172 eV which can be described as particle-hole transitions where the particle orbitals possess significant LF character as observed in the particle orbitals in figures 4 & 5 (inlaid; top left), a feature common with trigonal bipyramidal $Fe(CO)_5$.

These hypothesised crossings agree well with the potential energy curves shown in figures 4 & 5 with the lowest energy repulsive, 1E’ state of both axial and equatorial stretching (constructed from the $1A_1$’ and $1A_2$’ states in figure 4) as well as the second LF state, 2E”, crossing with the $1A_2$” bright MLCT state at minimal axial stretch (approx. 1.9 Å) and equatorial stretch (approx. 2.0 Å) distances. These stretches result in an axial ground state asymptote of 1.860 eV and equatorial ground state asymptote of 1.139 eV, resulting in the 1E’ state converging to an energy gap of 1.7457 and 1.7780 eV for the axial and equatorial stretches, respectively. Following dissociation, the ground and 1E’ states converge to a tetrahedral geometry through bending to fill in the coordination hole.[14, 44]

Our results for the two-photon absorption spectrum of $Fe(CO)_5$ are presented in table 3. As already discussed above, the two-photon absorption spectrum has never been investigated theoretically. Experimentally, two-photon absorption could be interesting as it enables a higher lying excited state could be probed using two photons of lower energy, as opposed to one photon of high energy that may be more difficult to produce. Two photon excitation has already been used to trigger the ultrafast photodissociation of $Fe(CO)_5$ in which the authors excited with

Table 3: *Coupled cluster response hierarchy for two-photon excited singlet states of $Fe(CO)_5$. Two-photon absorption transition strength for a pair of linear parallel polarized photons.*

QR-CCS			QR-CC2			QR-CCSD		
State	Excitation Energy (eV)	δ^{TP} (au)	State	Excitation Energy (eV)	δ^{TP} (au)	State	Excitation Energy (eV)	δ^{TP} (au)
1E’	4.040	1.3051	1E’	3.609	180.5155	1E’	4.385	0.0248
$1A_1$”	3.843	0.0000	$1A_1$”	4.385	0.0000	$1A_1$”	4.669	0.0000
1E”	3.836	0.2825	1E”	3.545	11.3715	1E”	4.842	1.1727
$1A_2$’	3.821	0.0000	$1A_2$’	3.749	0.0000	$1A_2$’	5.164	0.0000
2E”	4.197	2.7121	2E”	4.290	8.7837	2E”	5.174	0.8753
2E’	4.271	9.6605	2E’	3.689	2.6467	2E’	5.220	1.4881
$1A_2$”	4.767	0.0000	$1A_2$”	3.977	0.0000	$1A_2$”	5.233	0.0000
3E”	6.410	1.2949	3E”	4.333	528.3960	3E”	5.391	16.2609
$2A_2$’	6.554	0.0000				$2A_2$’	5.731	0.0000
3E’	6.838	48.7147	3E’	3.910	226.1020	3E’	5.753	25.2790
$1A_1$’	5.721	485.0950	$1A_1$’	3.753	14.1785	$1A_1$’	5.758	141.7180
$2A_1$’	6.976	2063.8725				$2A_1$’	5.939	17.6226
$2A_1$”	5.965	0.0000				$2A_1$”	6.352	0.0000
$2A_2$”	6.279	0.0000				$2A_2$”	6.419	1.2566
			4E’	4.158	1.0250			
			4E”	4.368	628.4248			

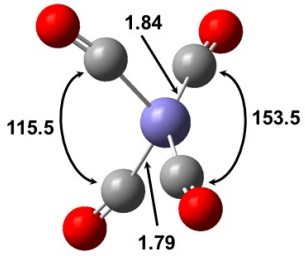

Figure 6: *C_{2v} equilibrium geometry of $Fe(CO)_5$;bond lengths in Å; angles in degrees*

two 3.1 eV energy photons,[8] a higher (total) energy of excitation compared to one photon absorption experiments (4.64 eV).[16] The two-photon absorption (TPA) electronic spectrum of $Fe(CO)_5$ is rich in spectral detail with many allowed states throughout the investigated range up to 7.2 eV.

The lowest energy TPA populated excited states are the 1E' and $1A_1$" states of LF and MLCT character, respectively. These compare well with results of Rubner *et al* [24] but the excitation energy values are slightly higher (for example, 3.98 eV with CASSCF compared to 4.409 eV with CCSD). After these two

Table 4: *LR-CCSD excited singlet states of $Fe(CO)_4$.*

State	Character	Excitation Energy (eV)	Oscillator Strength (au)
$1B_2$	LF ($3d_{yz}\rightarrow$) 41	1.0853	0.0070
$1A_1$	LF ($3d_{z^2}\rightarrow$) 40	1.6835	0.0122
$1B_1$	LF ($3d_{xz}\rightarrow$) 39	1.9584	0.0145
$1A_2$	LF ($3d_{xy}\rightarrow$) 38	2.5044	0.0000
$2B_2$	MLCT ($3d_{yz}\rightarrow \pi^*$)	329.61	0.0210
$2A_1$	MLCT ($3d_{z^2}\rightarrow \pi^*$)	4.2995	0.0334
$2B_1$	MLCT ($3d_{yz}\rightarrow \pi^*$ ‡‡)	4.3937	0.0367
$2A_2$	MLCT ($3d_{yz}\rightarrow \pi^*$ ‡‡) / ($3d_{z^2}\rightarrow \pi^*$ ‡‡)	4.4053	0.0000
$3B_2$	MLCT ($3d_{yz}\rightarrow \pi^*$ ‡‡)	4.6015	0.1014
$3A_1$	MLCT ($3d_{yz}\rightarrow \pi^*$ ‡‡)	4.6939	0.0237
$3A_2$	MLCT ($3d_{xy}\rightarrow \pi^*$) / ($3d_{yz}\rightarrow \pi^*$)	4.8043	0.0000
$3B_1$	MLCT ($3d_{xz}\rightarrow \pi^*$)	4.8123	0.0087
$4B_2$	MLCT ($3d_{z^2}\rightarrow \pi^*$ ‡‡)	4.9000	0.0018
$4A_2$	MLCT ($3d_{z^2}\rightarrow \pi^*$ ‡‡)	4.9914	0.0000
$4B_1$	MLCT ($3d_{z^2}\rightarrow \pi^*$ ‡‡) / LF ($3d_{xz}\rightarrow$)	5.0552	0.1093
$5A_2$	MLCT ($3d_{xy}\rightarrow \pi^*$) / ($3d_{yz}\rightarrow \pi^*$)	5.1644	0.0000
$4A_1$	MLCT ($3d_{xz}\rightarrow \pi^*$ ‡‡) / ($3d_{z^2}\rightarrow \pi^*$ ‡‡)	5.2337	0.0001
$5B_2$	MLCT ($3d_{xz}\rightarrow \pi^*$ ‡‡) / ($3d_{yz}\rightarrow \pi^*$ ‡‡)	5.2942	0.0106
$6A_2$	MLCT ($3d_{xz}\rightarrow \pi^*$ ‡‡)	5.5356	0.0000
$6B_2$	MLCT ($3d_{xz}\rightarrow \pi^*$ ‡‡)	5.5725	0.0094

‡‡ indicates an orbital of predominantly π* character containing significant *d* mixed character

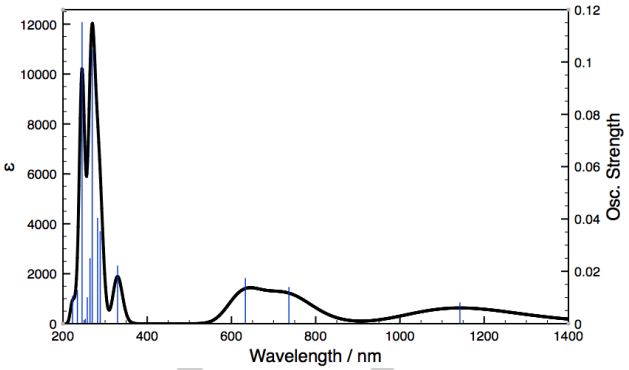

Figure 7: *LR-CCSD one-photon absorption spectra of $Fe(CO)_4$.*

states the spectrum is mostly dominated by MLCT transitions, also in agreement with the CASSCF/MR-CCI report and experiment.[31] The values of δ^{TPA} in the lower energy part of the spectrum are quite low until just above 5 eV where states with larger δ^{TPA} appear. The spectrum is dominated by the $1A_1'$ MLCT transition which has a δ^{TPA} value of 141 au, with other allowed transitions having lower, but still significant, δ^{TPA} values. The sheer number of allowed excited states within the investigated spectral range points towards some promising features of using two photon absorption techniques on $Fe(CO)_5$. From these results, it should be possible to excite $Fe(CO)_5$ into a manifold of MLCT states, all of different character and many of them degenerate. Should a degenerate state be directly populated or populated through ultrafast internal conversion from a non-degenerate state that is close in energy (for example $1A_1$' and 3E′) then this could cause Jahn-Teller distortions in the Franck-Condon region due to the system coupling to some non-totally symmetric molecular vibration. The results of the work of the two photon absorption experiment in Ref. [8], in which $Fe(CO)_5$ was excited at an energy of 6.20 eV are consistent with this and our calculated TPA . From the magnitude of the transition strengths in spectrum around the energy of the $2A_1'$ MLCT state appears likely to be the state populated in that experiment, although the excitation energy value is slightly lower at 5.939 eV. Other states could be possible that are close in energy to 6.20 eV but with lower TPA transition strengths, such as the $2A_2$" MLCT state at 6.419 eV. While excitation to both of these states is possible, it is clear that both states have MLCT character with slight LF mixed character.

After proceeding through a tetrahedral triply-degenerate conical intersection ($T \otimes t \oplus e$ type) $Fe(CO)_4$ in principle will attain one of eight equivalent structures of C_{2v} symmetry (see figure 6).[14, 44] However given the vibrationally hot nature of the $Fe(CO)_4$ it could easily pseudo-rotate around the Jahn-Teller

moat. It may then undergo thermalized dissociation to $Fe(CO)_3$. This intermediate $Fe(CO)_4$ may also undergo a sequential second one-photon absorption and we have calculated the vertical excited states from the structure shown in figure 6. These are presented as model absorption spectrum in figure 7 using the data in table 4. The spectral overlap with $Fe(CO)_5$ means that a sequential excited state absorption may be a route to further dissociation (at the limits of time-resolved TPA carried out to date).

Conclusions

We have applied for the first time a correlated coupled cluster response approach to investigate the one- and two-photon absorption of $Fe(CO)_5$ leading to dissociative photochemistry. There is a high degree of state mixing within a large density of states but CC response theory allows for identification of the optically active states and their potential crossings leading to reactive photochemistry. We have also shown the importance of correlation effects for this paradigm transition metal complex.

Computational Details

$Fe(CO)_5$ was optimised with D_{3h} molecular symmetry in its $^1A_1'$ ground state at the CCSD level of theory with a cc-pVDZ basis set. One- and two-photon absorption were calculated using linear and quadratic response theory with the CCS, CC2[45], and CCSD hierarchy. CCS is equivalent to configuration interaction singles (CIS). The intermediate model CC2 represents a lower cost approximation to CCSD, obtained by keeping only the lowest non-vanishing order term(s) from perturbation theory, and enforcing singles to be treated as zeroth-order, both with and without the external perturbation, via a T1 similarity transformation of all operators in the CC equations. LR-CC theory is closely related to the equation of motion (EOM) approach, being formally equivalent for excitation energies when compared to complete models, such as CCSD and CCSDT. Transition moments are more accurate with LR-CC,[46] although the difference is often negligible.[47] We have performed rigid scans along the axial and equatorial photodissociation coordinates for all states up to 7 eV using the EOM-CCSD formalism to characterise the states. Two-photon absorption was calculated via the single-residue of the quadratic response (QR) function. All results quoted are for a pair of linear parallel polarized photons of equal energy. The two-photon transition strength δ^{TPA} is given in atomic units and is proportional to the two-photon absorption cross-section. The all electron cc-pVTZ basis was used for all atoms in the excited state calculations. LR- and QR-CCSD calculations were performed using Dalton 2015,[48,49] while EOM-CCSD calculations were performed using Gaussian 16.[50,51] With $Fe(CO)_5$ at its D_{3h} ground state geometry, states of A_2'' and E' symmetry are allowed after absorption of one-photon whereas states of A_1', E' and E'' symmetry are allowed after absorption of two-photons. This indicates possible spectral overlap between one- and two-photon spectra possible through E' symmetry states.

Acknowledgements

MJP thanks EPSRC for funding through the platform grant EP/P001459/1, while TM thanks the EPRSC for support through a DTP studentship.

Keywords: inorganic photochemistry • theoretical spectroscopy • response theory • photodissociation • coupled cluster theory

References

[1] G. L. Geoffrey, M. S. Wrighton, *Organometallic Photochemistry*. **1979**, New York: Academic Press.
[2] M. Wrighton, *Chem Rev*, **1974**, 74, 401-430.
[3] N. A. Beach, and H.B. Gray, *J Am Chem Soc*, **1968**, 90, 5713-5721.
[4] M. A. Graham, A. J. Rest, J. J. Turner, *J Organomet Chem*, **1970**. 24, C54-C56.
[5] R. A. Levenson, H. B. Gray, G. P. Ceasar, *J Am Chem Soc*, **1970**, 92, 3653-3658.
[6] T. R. Fletcher, R. N. Rosenfeld, *J Am Chem Soc*, **1983**, 105, 6358-6359.
[7] R. L. Whetten, K. J. Fu, E. R. Grant, *J Chem Phys*, **1983**, 79, 4899-4911.
[8] L. Banares, T. Baumert, M. Bergt, B. Kiefer, G. Gerber, *Chem Phys Lett*, **1997**, 267, 141-148.
[9] M. Gutmann, J. M. Janello, M. S. Dickebohm, M. Grossekathöfer, J. Lindener-Roenneke, *J Phys Chem A*, **1998**, 102, 4138-4147.
[10] H. Ihee, J. Cao, A. H. Zewail, *Chem Phys Lett*, **1997**, 281, 10-19.
[11] S. K. Kim, S. Pedersen, A. H. Zewail, *Chem Phys Lett*, **1995**, 233, 500-508.
[12] O. Rubner, V. Engel, *Chem Phys Lett*, **1998**, 293, 485-490.
[13] S. A. Trushin, W. Fuss, W. E. Schmid, K. L. Kompa, *J Phys Chem A*, **1998**, 102, 4129-4137.
[14] R. J. Mckinlay, J. M. Żurek, M. J. Paterson, *Adv. Inorg. Chem*., **2010**, 62, 351.
[15] W. Fuss, S. A. Trushin, W. E. Schmid, *Res Chem Intermediat*, **2001**, 27, 447-457.
[16] S. A. Trushin, W. Fuss, K. L. Kompa, W. E. Schmid., *J Phys Chem A*, **2000**, 104, 1997-2006.
[17] S. A. Trushin, W. Fuss, W. E. Schmid, *Chem Phys*, **2000**, 259, 313-330.
[18] S. A. Trushin, K. Kosma, W. Fuß, W. E. Schmid, *Chem Phys*, **2008**, 347, 309-323.
[19] S. Villaume, A. Strich, C. Daniel, S. A. Perera, R. J. Bartlett, *Phys Chem Chem Phys*, **2007**, 9, 6115-6122.
[20] C. Daniel, M. Benard, A. Dedieu, R. Wiest, A. Veillard, *J Phys Chem*, **1984**, 88, 4805-4811.
[21] O. Kuhn, M. R. D. Hachey, M. M. Rohmer, C. Daniel, *Chem Phys Lett*, **2000**, 322, 199-206.
[22] A. Marquez, C. Daniel, J. F. Sanz, *J Phys Chem*, **1992**, 96, 121-123.
[23] B. J. Persson, B. O. Roos, K. Pierloot, *J Chem Phys*, **1994**, 101, 6810-6821.
[24] O. Rubner, V. Engel, M. R. D. Hachey, C. Daniel, *Chem Phys Lett*, **1999**, 302, 489-494.
[25] O. Christiansen, *Theor Chem Acc*, **2006**, 116, 106-123.
[26] N. Leadbeater, *Coordin Chem Rev*, **1999**, 188, 35-70.
[27] M. Schreiber, M. R. Silva-Junior, S. P. A. Sauer, W. Thiel, *J. Chem. Phys*., **2008**, 128, 134110
[28] M. R. Silva-Junior, S. P. A. Sauer, M. Schreiber, W. Thiel, *Mol. Phys*., **2010**, 108, 453.
[29] M. J. Paterson, O. Christiansen, F. Pawłowski, P.Jørgensen, C. Hättig, T. Helgaker, P. Sałek, *J. Chem. Phys*., **2006**, 124, 054322.
[30] N. M. S. Almeida, R. G. McKinlay, M. J. Paterson, *Chem Phys,* **2015**, 446, 86.
[31] M. Kotzian, N. Roesch, H. Schroeder, M. C. Zerner, *J Am Chem Phys*, **1989**, 111, 7687-7696.
[32] B. Dick, H. J. Freund, G. Hohlneicher, *Mol Phys*, **1982**, 45, 427-439.
[33] K. Pierloot, B. Dumez, Widmark P-O, Roos B. O., *Theor Chim Acta*, **1995**, 90, 149-181.

[34] J. T. Yardley, B. Gitlin, G. Nathanson, A. M. Rosan, *J Chem Phys*, **1981**, 74, 370-378.
[35] T. A. Seder, A. J. Ouderkirk, E. Weitz, *J Chem Phys*, **1986**, 85, 1977-1986.
[36] A. Veillard, A. Strich, C. Daniel, P. E. M. Siegbahn, *Chem Phys Lett*, **1987**, 141, 329-333.
[37] H. Ihee, J. M. Cao, A. H. Zewail, *Angew Chem Int Edit*, **2001**, 40, 1532.
[38] M. Poliakoff, J. J. Turner, *Angew Chem Int Edit*, **2001**, 40, 2809-2812.
[39] A. Rosa, E. J. Baerends, S. J. A. van Gisbergen, E. van Lenthe, J. A. Groeneveld, J. G. Snijders, *J Am Chem Soc*, **1999**, 121, 10356-10365.
[40] B. Beagley, D. G. Schmidling, *J. Mol. Struct.*, **1974**, 22, 466.
[41] D. Braga, F. Grepioni, A. G. Orpen, *Organometallics*, **1993**, 12, 1481.
[42] R. G. Mckinlay, N. M. S. Almeida, J. P. Coe, M. J. Paterson, *J. Phys. Chem. A*, **2015**, 119, 10076.
[43] D. J. Taylor, M. J. Paterson, *J. Chem. Phys.*, **2010**, 133, 204302.
[44] R.G. Mckinlay, M. J. Paterson, *The Jahn-Teller Effect in Binary Transition Metal Carbonyl Complexes, in The Jahn Teller Effect: Advances and Perspectives*, H. Koppel, H. Barentzen, and D.R. Yarkony, Editors. **2009**, Springer-Verlag: Heidelberg.
[45] H. Koch, R. Kobayashi, A. Sanchez de Meras, P. Jørgensen, *Chem. Phys. Lett.*, **1995**, 243, 409-418.
[46] H. Koch, R. Kobayashi, A. Sanchez de Meras, P. Jørgensen, *J. Chem. Phys.* , **1994**, 100, 4393-4400.
[47] M. Caricato, G.W. Trucks, M. J. Frisch, *J Chem Phys.* , **2009**. 131: p. 174104.
[48] K. Aidas, C. Angeli, K. L. Bak, V. Bakken, R. Bast, L. Boman, O. Christiansen, R. Cimiraglia, S. Coriani, P. Dahle, E. K. Dalskov, U. Ekström, T. Enevoldsen, J. J. Eriksen, P. Ettenhuber, B. Fernández, L. Ferrighi, H. Fliegl, L. Frediani, K. Hald, A. Halkier, C. Hättig, H. Heiberg, T. Helgaker, A. C. Hennum, H. Hettema, E. Hjertenæs, S. Høst, I.-M. Høyvik, M. F. Iozzi, B. Jansik, H. J. Aa. Jensen, D. Jonsson, P. Jørgensen, J. Kauczor, S. Kirpekar, T. Kjærgaard, W. Klopper, S. Knecht, R. Kobayashi, H. Koch, J. Kongsted, A. Krapp, K. Kristensen, A. Ligabue, O. B. Lutnæs, J. I. Melo, K. V. Mikkelsen, R. H. Myhre, C. Neiss, C. B. Nielsen, P. Norman, J. Olsen, J. M. H. Olsen, A. Osted, M. J. Packer, F. Pawlowski, T. B. Pedersen, P. F. Provasi, S. Reine, Z. Rinkevicius, T. A. Ruden, K. Ruud, V. Rybkin, P. Salek, C. C. M. Samson, A. Sánchez de Merás, T. Saue, S. P. A. Sauer, B. Schimmelpfennig, K. Sneskov, A. H. Steindal, K. O. Sylvester-Hvid, P. R. Taylor, A. M. Teale, E. I. Tellgren, D. P. Tew, A. J. Thorvaldsen, L. Thøgersen, O. Vahtras, M. A. Watson, D. J. D. Wilson, M. Ziolkowski, H. Ågren, "The Dalton quantum chemistry program system", WIREs *Comput. Mol. Sci*. **2014**, 4:269–284.
[49] Dalton, a molecular electronic structure program, Release DALTON2014.0 (**2015**), see http://daltonprogram.org
[50] Gaussian 16 Revision A.03, M. J. Frisch, G. W. Trucks, H. B. Schlegel, G. E. Scuseria, M. A. Robb, J. R. Cheeseman, G. Scalmani, V. Barone, G. A. Petersson, H. Nakatsuji, X. Li, M. Caricato, A. V. Marenich, J. Bloino, B. G. Janesko, R. Gomperts, B. Mennucci, H. P. Hratchian, J. V. Ortiz, A. F. Izmaylov, J. L. Sonnenberg, D. Williams-Young, F. Ding, F. Lipparini, F. Egidi, J. Goings, B. Peng, A. Petrone, T. Henderson, D. Ranasinghe, V. G. Zakrzewski, J. Gao, N. Rega, G. Zheng, W. Liang, M. Hada, M. Ehara, K. Toyota, R. Fukuda, J. Hasegawa, M. Ishida, T. Nakajima, Y. Honda, O. Kitao, H. Nakai, T. Vreven, K. Throssell, J. A. Montgomery, Jr., J. E. Peralta, F. Ogliaro, M. J. Bearpark, J. J. Heyd, E. N. Brothers, K. N. Kudin, V. N. Staroverov, T. A. Keith, R. Kobayashi, J. Normand, K. Raghavachari, A. P. Rendell, J. C. Burant, S. S. Iyengar, J. Tomasi, M. Cossi, J. M. Millam, M. Klene, C. Adamo, R. Cammi, J. W. Ochterski, R. L. Martin, K. Morokuma, O. Farkas, J. B. Foresman, D. J. Fox, Gaussian, Inc., Wallingford CT, **2016**.
[51] GaussView, Version 6, Roy Dennington, Todd A. Keith, John M. Millam, Semichem Inc., Shawnee Mission, KS, **2016**.

10.1002/cptc.201900111

WILEY-VCH

ARTICLE

Entry for the Table of Contents (Please choose one layout)

Layout 1:

ARTICLE

One- and two-photon induced dissociative photochemistry in $Fe(CO)_5$

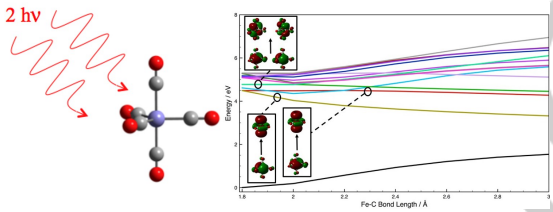

*Author(s), Corresponding Author(s)**

Page No. – Page No.

Title

Layout 2:

ARTICLE

((Insert TOC Grapic here))

*Author(s), Corresponding Author(s)**

Page No. – Page No.

Title

Text for Table of Contents